Mineral Liberation and the Batch Comminution Equation

R.P. King and C.L. Schneider
Comminution Center
University of Utah
Salt Lake City UT 84112

ABSTRACT

The batch comminution equation for multicomponent mineral systems is a multidimensional integrodifferential equation

$$\frac{\partial P(g,D;t)}{\partial t} = \iint_{R'} S(g',D')\,B(g,D\,|\,g',D')\,p(g',D';t)\,dg'dD'$$

that cannot be solved analytically. The phase space (g, D) is usually discretized and the equation is formulated as

$$\frac{dp_{ij}}{dt} = -S_{ij}p_{ij} + \sum_{l=1}^{j-1}\sum_{k=K_l^*}^{K_l^{**}} S_{kl}\; b_{ijkl}\; p_{kl}$$

Solutions to this discretized form of the equation are easy to generate provided that models for the selection function S_{ij} and the multicomponent breakage function b_{ijkl} are known.

An assumption of random fracture provides an important simplification because, under the random fracture assumption, the selection function is independent of the particle composition. The random fracture assumption has often been used by researchers who developed models for the prediction of mineral liberation by comminution and the solution of the batch comminution equation under this assumption was found to be

$$p_{ij}(t) = \sum_{l=1}^{j} A_{ijl}e^{-S_l t}$$

with the coefficients given by

$$A_{ijj} = p_{ij}(0) - \sum_{i=1}^{j-1} A_{ijl}$$

and

$$A_{ijn} = \frac{\sum_{l=n}^{j-1} S_l \sum_{k=1}^{12} b_{ijkl}A_{kln}}{S_j - S_n}$$

A general solution to the batch comminution equation that does not rely on the random fracture assumption is also derived in the paper and is given by

$$p_{ij} = \sum_{l=1}^{j} \sum_{k=1}^{12} \alpha_{ijkl} e^{-S_{kl} t}$$

with the coefficients given by

$$\alpha_{ijmj} = 0 \qquad \text{if} \quad i \neq m$$

$$\alpha_{ijij} = p_{ij}(0) - \sum_{l=1}^{j-1} \sum_{k=1}^{12} \alpha_{ijkl}$$

$$\alpha_{ijmn} = \frac{\sum_{l=n}^{j-1} \sum_{k=1}^{12} S_{kl}\, b_{ijkl}\, \alpha_{klmn}}{S_{ij} - S_{mn}}$$

The new solution was compared with experimental data obtained from a batch test on a difficult-to-liberate ore. The model was found to be reliable and the derived Andrews-Mika diagram is shown.

The derived models for the selection function and the Andrews-Mika diagram can be used to simulate the effects of the non random fracture, and thus to assess their relative importance, and also to simulate the behavior of the ore in continuous milling and concentrating circuits.

INTRODUCTION

The population balance equation for batch milling

$$\frac{\partial P(D;t)}{\partial t} = \int_{D}^{\infty} S(y)\, B(D \mid y)\, p(y;t)\, dy \tag{1}$$

can be solved analytically (King, 1972, Nakajima and Tanaka, 1973) for a few specific selection and breakage functions when it is not necessary to account for the liberation of the mineral phases during comminution. Practical solutions are usually generated using a finite collection of ordinary differential equations that are generated by discretization of the size coordinate.

$$\frac{dp_j}{dt} = -S_j p_j + \sum_{l=1}^{j-1} S_l b_{jl} p_l \tag{2}$$

When the ore is heterogeneous the liberation of the individual mineral phases becomes important and the batch comminution equation must be modified accordingly. The modifications that are required to apply this equation to binary ores were comprehensively investigated by Andrews and Mika in 1975 who wrote the equation in terms of the particle assay and the particle mass (a, m)

$$\frac{\partial F(a,m;t)}{\partial t} = \iint_{R'} S(\alpha,\mu) B(a,m \mid \alpha,\mu)\, f(\alpha,\mu;t)\, d\alpha\, d\mu \tag{3}$$

In equation (3), $F(a,m;t)$ is the fraction by mass in the mill charge at time t that consists of particles having individual masses less than or equal to m and individual assays less than or equal to a. The cumulative breakage function $B(a,m \mid \alpha,\mu)$ is the fraction by mass of the progeny with essay $\leq a$ and mass $\leq m$ that results from the fracture of a parent particle of mass μ and assay α.

Analytical solutions to equation (3) are not available except for systems that are severely and unrealistically restricted. Numerical methods are the only practical possibility for generating useful solutions. A convenient solution method is presented here.

THE ANDREWS-MIKA DIAGRAM AND ITS SIGNIFICANCE

The double integral in equation (3) is taken over a region R' in the particle mass, particle composition space. This region contains all parent particles that can generate a progeny particle of mass m and composition a. The region R' does not comprise the entire half space $\mu \geq m$ but is restricted by mass conservation and mineralogical texture constraints. The significance of these restrictions was pointed out by Andrews and Mika in 1975 and the determination of these constraints is important when solutions to equation (3) are generated.

Andrews and Mika established the following conservative bounds for the region R'

$$\mu \geq m \tag{4}$$

and

$$\begin{aligned} \alpha\mu &\geq am \\ (1-\alpha)\mu &\geq (1-a)m \end{aligned} \tag{5}$$

These bounds reflect the obvious requirement that the parent particle must be at least as large as any of its progeny and that the mass of mineral in the parent particle must be at least as large as the mass of mineral in any progeny particle. R' is bounded above by the mass of the largest particle in the mill feed (m_{max}). The region R' is illustrated in Figure 1 where point A represents the composition and mass of any progeny particle. The boundaries of R' never intersect the vertical axes at $a = 0$ and $a = 1.0$ because of the obvious fact that a completely liberated parent cannot produce any unliberated progeny.

A region R, complementary to R', can also be defined. If point A in Figure 1 represents the mass and composition of a parent particle, region R is the attainable region for progeny that results when the parent is broken in the mill. R' is called the feeder region for progeny at point A and R is called the attainable region from a parent at point A. The boundaries of R are continuations of the boundary lines of R' and are obtained by reversing inequalities (4) and (5).

$$m \leq \mu \tag{6}$$

and

$$\begin{aligned} am &\leq \alpha\mu \\ (1-a)m &\leq (1-\alpha)\mu \end{aligned} \tag{7}$$

Unlike the boundaries of R', those of R intersect the vertical axes $a = 0$ and $a = 1$ at points B and C respectively. These intersection points reflect the conservation law: "The mass of the largest possible liberated progeny particle is equal to the mass of the mineral phase contained in the parent particle". Point B is defined when this principle is applied to the gangue and point C when it is applied to the mineral phase. The segments BF and CG are attainable from the point A because a particle of mass m and grade a can produce progeny consisting of pure gangue provided that the mass of the liberated gangue particle is less than the mass of the gangue phase in the parent particle (equal to $(1-a)m$). Likewise a progeny particle consisting of pure mineral can be produced from a parent particle at (a,m) if the mass of the liberated daughter is less then the mass of the mineral phase in the parent.

In practice the particle-mass, particle-assay coordinate system is not practical for population balance modeling applications and the particle-size, particle-composition system is used instead. This preference expresses the fact that it is much easier to classify particles on the basis of size than on the basis of the mass of individual particles. When particle size is used rather than particle mass, equation (3) is written

$$\frac{\partial P(g,D;t)}{\partial t} = \iint_{R'} S(g',D')\,B(g,D\,|\,g',D')\,p(g',D';t)\,dg'dD' \tag{8}$$

The Andrews-Mika diagram in the particle-size particle-composition space has the same essential characteristics as that in the mass-composition space. However, the inequalities (9) to (7) that define the boundaries of the feeder and attainable regions cannot be written in precise form and the following approximations are used

$$g\ D^3 \leq g'D'^3 \tag{9}$$

for the mineral and

$$(1-g)D^3 \leq (1-g')D'^3 \tag{10}$$

for the gangue.
In fact these boundaries become fuzzy (in the sense of fuzzy set theory) because a population of particles of equal mass or volume have a distribution of sizes if the particles are of irregular shape. This fuzziness is neglected in this paper.

The constraints expressed by inequalities (9) and (10) are in most cases conservative and tighter bounds on the regions R and R' can be established by careful evaluation of experimental data.

To see this, consider point E in Figure 1. This point reflects the principle that the largest completely

liberated mineral progeny particle that can be formed cannot be larger than the single largest coherent mineral grain in the parent particle. The largest coherent grain is generally smaller than the total volume of mineral phase in the parent depending on the mineralogical texture. If the parent particle contains more than one grain of mineral, the largest liberated progeny particle can be no larger than the largest simple mineral grain in the parent particle. If the texture is fine grained relative to the size of the parent particle, no large completely liberated particle can result from breakage and the corner E of the attainable region must lie well below point *C* and the upper boundaries of region *R* will lie below lines *AC* and *AB* in Figure 1.

In addition to its important boundary structure, the Andrews-Mika diagram also has internal structure which is defined as the value of the function

$$b(g,D|\,g',D') \;=\; \frac{\partial^2 B(g,D|\,g',D')}{\partial g\,\partial D} \tag{11}$$

This function describes the density of arrival of progeny particles at point (g,D) in R from breakage of a parent at (g',D'). Because the cumulative function $B(g,D|g',D')$ has step discontinuities at $g = 0$ and $g = 1$, the function $b(g,D|g',D')$ has Dirac delta functions at $g = 0$ and at $g = 1$. The strength of these delta functions represent the liberated gangue and mineral respectively.

The internal structure of the Andrews-Mika diagram is subject to additional constraints since in any grinding mill the total amounts of each mineral over all the sizes are conserved. A sufficient condition that ensures phase conservation is

$$\int_0^{D'}\int_0^1 g\;\; b(g,D|g',D')\,dg\,dD \;=\; g' \qquad \text{for every } g' \text{ and } D' \tag{12}$$

This condition is derived in the appendix. This condition is particularly useful in the following form

$$\int_0^{D'} b(D|g',D')\int_0^1 g\,b(g|D,g',D')\,dg\,dD \;=\; g' \tag{13}$$

Before solutions of the batch comminution equation for multi-component materials can be generated, the function $b(g,D|g',D')$ must be available. This requires a complete set of Andrews-Mika diagrams for the ore in question.

DISCRETE PHASE SPACE

The integrodifferential equation (8) can be solved numerically using a comparatively coarse grid to discretize the phase space. Typically the size coordinate is discretized using a $\sqrt{2}$ geometrical sequence and the particle grade is discretized into 12 classes - one for the liberated gangue, one for the liberated mineral and 10 equally spaced intervals in the range from $g = 0$ to $g = 1$.

In the discrete form, equation (8) becomes

$$\frac{dp_{ij}}{dt} = -S_{ij}p_{ij} + \sum_{l=1}^{j-1} \sum_{k=K_l^*}^{K_l^{**}} S_{kl}\, b_{ijkl}\, p_{kl} \tag{14}$$

In equation (14) i,j,k and l index the variables g, D, g' and D' respectively. K_l^* and K_l^{**} are the left and right hand boundaries of region R' for parent particles in size class l. b_{ijkl} is the discretized version of the function $b(g,D|g',D')$. Early attempts (Wiegel, 1976, Choi *et. al.*1988) to use equation (14) foundered because of the complexity of the function b_{ijkl}. Practical solutions were developed only for the unrealistically simplified case of three particle compositions; liberated mineral, liberated gangue and all unliberated particles lumped together. This is commonly referred to as the "A, A-B, B" model. This model has not found much application in practice because it fails to generate any really useful information about the liberation that is achieved during milling.

In practice it is convenient to decouple the size reduction process from the liberation process. This can be done by using the conditional breakage functions

$$b_{ijkl} = b_{j,kl}\; b_{i,jkl} \tag{15}$$

where $b_{j,kl}$ is the fraction of material breaking from class k,l that reports to size class j. $b_{i,jkl}$ is the conditional transfer coefficient from grade class k to grade class i given that the particle transfers from size class l to size class j. $b_{i,jkl}$ is usually represented as an Andrews-Mika diagram. $b_{j,kl}$ and $b_{i,jkl}$ are conditional distributions and must satisfy the conditions

$$\sum_{j=l+1}^{N} b_{j,kl} = 1 \tag{16}$$

and

$$\sum_{i=1}^{12} b_{i,jkl} = 1 \tag{17}$$

Typical examples of the discretized Andrews-Mika diagram are shown in Figures 2 and 3. It is important to realize that these represent just two of the many discrete Andrews-Mika diagrams that are required to characterize any particular ore. Figures 2 and 3 show a discretization over 19 size classes and 12 grade classes which requires 19×12 = 228 separate Andrews-Mika diagrams, one for each possible combination of k and l. In general a theoretical model of the Andrews-Mika diagram is required to generate the appropriate matrices which can be stored before the solution to the batch comminution equation is generated. The Andrews-Mika diagrams in Figures 2 and 3 were generated using a model for the attainable region that was developed by Schneider (1995). A useful approximation results when it is assumed that the Andrews-Mika diagram is normalized with respect to particle size so that $b_{i,jkl}$ is a function only of the difference l-j when the size scale is discretized in geometric progression. This is equivalent to a normalization based on the ratio of sizes. This approximation will be valid only over comparatively small size ranges. However, when this

assumption is made, only twelve Andrews-Mika diagrams are required for a complete characterization of the breakage process. The two attainable regions for liberated parents are trivial and easy to construct. This leads to a manageable parameterization of the problem.

The attainable region is significantly easier to model than the feeder region because the attainable region has such a clearly definable structure. However the feeder regions can be synthesized from a complete collection of attainable regions in the following way. Let $a_{m,nuv}$ represent the attainable regions for parents at u,v . Then the feeder regions are generated from

$$b_{i,jkl} = a_{k,jil} \tag{18}$$

Once all the Andrews-Mika diagrams have been constructed for the ore in question, equation (15) can be used to calculate the coefficients b_{ijkl} from the size breakage function and solutions to the batch comminution equation (14) can be addressed.

SOLUTION OF THE DISCRETE BATCH COMMINUTION EQUATION

The numerical solution of equations (14) is not difficult. The differential equations can be integrated numerically in sequential order starting with p_{11} and then incrementing the index i over the range 1 to 12 for each successive value of the index j.

The summation on the right hand side of equation (14) is taken over the region R' in the Andrews-Mika diagram. It is necessary to construct R' from R or to design an algorithm that runs the summation over R rather than R'. A suitable algorithm is not difficult to develop. (King, 1990, King and Schneider, 1993).

When generating analytical solutions to equation (14), it is more convenient to construct R' from R and then exploit the linearity of the differential equations (14) to generate the general solution

$$p_{ij} = \sum_{l=1}^{j} \sum_{k=1}^{12} \alpha_{ijkl} e^{-S_{kl} t} \tag{19}$$

The coefficients in equation (19) are related to the selection and breakage functions and to the initial conditions using the following recursion relationships

$$\alpha_{ijmj} = 0 \qquad \text{if } i \neq m \tag{20}$$

$$\alpha_{ijij} = p_{ij}(0) - \sum_{l=1}^{j-1} \sum_{k=1}^{12} \alpha_{ijkl} \tag{21}$$

$$\alpha_{ijmn} = \frac{\sum_{l=n}^{j-1} \sum_{k=1}^{12} S_{kl} \; b_{ijkl} \alpha_{klmn}}{S_{ij} - S_{mn}} \tag{22}$$

Note that the summations in equation (22) run over the feeder regions and not over the attainable regions.

This solution to equation (14) is based on the usual convention that breakage implies that all progeny leave the size class of the parent particle. The pathological case $S_{ij} = S_{mn}$ is occasionally encountered in practice. When it occurs, it is usually handled by making a slight adjustment to the parameters that define the relationship between the specific rate of breakage and the particle size to assure that no two values of S_{ij} are exactly equal.

Equation (19) represents a complete and convenient solution to the discrete version of the batch comminution equation with liberation and this solution produces the size distribution as well as the liberation distribution as a function of the time of grinding.

SIMPLIFICATIONS OF THE SOLUTION DUE TO RANDOM FRACTURE

Several simplifying assumptions can be made that facilitate the generation of practical solutions and which reduce the amount of experimental work that is necessary to characterize the coefficients S_{ij} and b_{ijkl}.

The random fracture assumption is often invoked because it simplifies any model of mineral liberation. Under this assumption the fracture pattern that results during comminution of any particle is independent of the mineralogical composition and texture of the particle. The random fracture model leads to several useful simplifications of the multi-component batch comminution equation and these are discussed in this section.

The following six conditions characterize random fracture.

1. No **selective breakage.** The effects of unequal brittleness of the mineral phases give rise to a number of different phenomena. Firstly the minerals break selectively which manifests itself as a variation of the selection function with mineral type and therefore particle composition. Selective breakage depends on the flaw size distribution and the fracture toughness of the material in accordance with the classic Griffiths model of fracture mechanics. Under the random fracture assumption, the mineral phases are equally brittle and the specific rate of breakage S_{ij} is therefore not a function of the composition of the parent particle. Thus

$$S_{ij} = S_j \tag{23}$$

which is a function only of the size of the parent particle. With this condition the general solution can now be written in terms of a smaller set of coefficients

$$A_{ijl} = \sum_{k=1}^{12} \alpha_{ijkl} \tag{24}$$

and is

$$p_{ij}(t) = \sum_{l=1}^{j} A_{ijl} e^{-S_l t} \tag{25}$$

The coefficients are obtained from

$$A_{ijj} = p_{ij}(0) - \sum_{l=1}^{j-1} A_{ijl} \tag{26}$$

$$A_{ijn} = \frac{\sum_{l=n}^{j-1} S_l \sum_{k=1}^{12} b_{ijkl} A_{kln}}{S_j - S_n} \tag{27}$$

which can be evaluated recursively.

2. No **differential breakage.** Differential breakage occurs when the *size* breakage function depends on the composition of the parent particle. This phenomenon differs from preferential breakage because it is function of the total composition and microstructural texture of the parent particle. Particles that are made up of minerals having different physical properties will contain high internal stresses Random fracture implies that differential breakage does not occur during comminution and the size breakage function $b_{j,kl}$ is independent of the composition of the parent particle. Then equation (15) becomes

$$b_{ijkl} = b_{j,l} \; b_{i,jkl} \tag{28}$$

3. No **preferential breakage.** Preferential breakage occurs when crack branching occurs more frequently in one mineral than in the others. This leads to the appearance of the preferentially broken mineral in the finer sizes after each elementary fracture event. Under the assumption of random fracture, no preferential breakage occurs and then the internal consistency condition (12) takes on the simple form

$$\sum_{i=1}^{12} g_i b_{i,jkl} = g_k \qquad \text{for all } k \text{ and } l. \tag{29}$$

Equation (29) ensures that the discrete version of equation (13) is always satisfied.

4. No **phase-boundary fracture.** Phase-boundary fracture is said to occur when cracks tend to propagate preferentially along phase boundaries rather than across the phases. Under the random

fracture assumption no phase-boundary fracture occurs. It is known (King, 1994) that phase-boundary fracture does not influence liberation significantly and therefore no special provision is made in the models of the attainable region to accommodate this effect.

5. No **liberation by detachment** (Gaudin, 1939, p77) When the grains of a particular mineral are comparatively loosely bonded into the ore matrix, the mineral grains become detached from the ore during grinding leading to significant liberation of the original mineral. These liberated mineral grains are concentrated around the mineral "grain size" in the progeny of any elementary fracture event. This effect can be incorporated into the models of the attainable region by increasing the concentration of the liberated mineral class in the regions of the mineral "grain-size". This would show up for example as a local peak in the bars in the 100% grade class in the Andrews-Mika diagram shown in Figure 2. In addition, the size breakage function must be modified to reflect the greater arrival rate of progeny particles in this size range. Liberation by detachment is an extreme form of phase-boundary fracture and it influences the liberation characteristics profoundly when it occurs.

6. No **boundary-region fracture.** The material in the neighborhood of a phase boundary can be highly stressed if the elastic moduli of the minerals differ significantly. This can lead to preferential fracture of both phases in the region of a phase boundary which in turn can lead to the generation of finer particles from that region. This type of fracture produces the interesting result that finer particles, originating from the phase-boundary region, are *less* liberated than coarser particles. This apparently anomalous result can be incorporated into the models of the attainable region as a shallow peak in the intermediate grade classes at the finest progeny sizes. This shows up as a slight bulge in these classes in the lowest rows of the Anrews-Mika diagram shown in Figure 2.

CALCULATED RESULTS - RANDOM FRACTURE

Twelve Andrews-Mika diagrams for the region R were generated using the model developed by Schneider and two typical diagrams are shown in Figures 2 and 3. The remaining diagrams are similar in character and are not shown here. The diagrams in each of the feeder regions were constructed from the complete set of attainable region diagrams using equation (18). Typical feeder regions with typical attainable regions are illustrated in Figures 2 and 3. The average selection function S_j was calculated using the usual Austin form

$$S_j = \frac{a\ d_p^{\alpha}}{1 + \left(\frac{d_p}{\mu}\right)^{\Lambda}} \tag{30}$$

and under the random fracture assumption, this selection function is independent of particle composition.

The size breakage function was calculated using

$$B(x,y) = \Phi\left(\frac{x}{y}\right)^{\beta} + (1-\Phi)\left(\frac{x}{y}\right)^{\gamma} \tag{31}$$

The liberation spectra, calculated using equation (25) are shown in Figure 4 after 10 minutes grinding of a monosize feed larger than the "liberation" size of the ore. The feed in this case was monosize unliberated material of average grade 36.8% mineral. The results shown in Figure 3 are plotted as conditional liberation spectra at each size. In other words the spectra are normalized so that they sum to unity at each size. The conditional liberation spectra do not change significantly with grinding time after the initial transient has died out. This results from the constraint imposed by equation (29). The average concentration of mineral phase does not vary with size in the product from the batch mill when random fracture is assumed.

CALCULATED RESULTS - NON-RANDOM FRACTURE

The general solution equation (19) can be used to illustrate the effect of non random fracture. Non random fracture can be caused by several effects as discussed in a previous section. The effects of selective breakage, preferential breakage and differential breakage are illustrated here.

Selective breakage can be simulated by defining the brittleness of each mineral species and modeling the selection function in terms of the brittleness ratio, *br*, as follows (King 1994, Middlemiss and King 1996).

$$S_{ij} = \frac{2\left(g_i + (1-g_i)br\right)S_{oj}}{1 + br} \tag{32}$$

Here S_{oj} is the average selection function of the ore at size class *j* which can be calculated, for example, using an Austin model (equation (30)).

Preferential breakage occurs when growing cracks branch more readily in one of the mineral phases. This mineral will appear preferentially in the smaller size classes during any elementary fracture event and its effects can be simulated by appropriate modifications to the internal and boundary structures of the attainable region. In particular the conditional mean

$$\bar{g}_{jkl} = \sum_{i=1}^{12} g_i b_{i,jkl} \tag{33}$$

can be allowed to vary appropriately with progeny size while still satisfying the required condition of equation (13) in discrete form namely

$$\sum_{j=0}^{N} \bar{g}_{jkl} b_{j,kl} = g_k \tag{34}$$

Schneider (1995) has proposed a useful model for this variation

$$\bar{g}_{jkl} = g_k \pm w(g_k)v(D_j/D_l) \tag{35}$$

with

$$\sum_{j=l+1}^{N} v(D_j/D_l)\, b_{j,kl} = 0 \qquad \text{for all} \quad k,l \tag{36}$$

Experimental data suggests a function of the form

$$v(u) = u^{\alpha}\ln(u) \tag{37}$$

with

$$u_{jl} = \frac{1 - D_j/D_l}{1 - \Delta_0} \tag{38}$$

The sign in equation (35) is selected depending on whether preferential breakage occurs in the mineral (+) or the gangue (-). The parameter Δ_0 can be easily adjusted to ensure that equation (36) is satisfied once the size breakage function has been established.

EXPERIMENTAL RESULTS

A monosize sample of ball mill feed was prepared from samples collected on an operating plant. This was used as the starting material for the batch mill test in a 25 cm diameter laboratory batch mill. Separate batch grinding experiments were run for 10, 20 and 30 minutes respectively. The products from the mill were screened and each screen fraction was sampled, mounted, sectioned and polished prior to image analysis using SEM with back-scattered electron detection as the image source. The linear intercept method was used to determine the distribution of linear grades in each size fraction. The linear grade distributions were stereologically corrected using the entropy regularization method (King and Schneider, 1998) to yield the experimental distributions p_{ij}. The results are shown in Figure 5.

Evidence of selective fracture was clearly visible in the liberation spectra measured after 10 minutes of grinding. Residual particles in the feed monosize and the sizes just smaller than the feed showed a definite shift to higher mineral grades during grinding indicating that the gangue was more brittle than the mineral phase and was breaking selectively. The batch equation was accordingly solved using a brittleness ratio of 0.5 and the calculated liberation spectra are shown in Figure 6.

The measured mineral concentration at each particle size is shown in Figure 7 . The decrease in the average grade as the particle size decreases is typical when the gangue is more brittle than the mineral phase. The concentration of mineral is larger than the original feed concentration in the feed monosize and in the size fractions immediately below the feed monosize. At all smaller sizes, the mineral concentration is smaller than the feed concentration as the more brittle gangue is selectively

ground and concentrates in the smaller sizes.

The calculated cumulative liberation over all sizes is shown in Figure 8 for equal brittleness of the two phases and in Figure 9 for a brittleness ratio of 0.5. There is no difference in these results when averaged over all sizes showing that there is no cumulative effect of selective breakage. This remarkable result shows that, when all sizes in the mill product are taken together, the total liberation spectrum is not affected by the relative brittleness of the individual minerals. The size-by-size variation of average particle composition nevertheless shows a marked variation as shown in Figure 7.

Evidence for preferential breakage of gangue during the comminution of iron ore by slow compression in a piston and die arrangement has been presented by Fandrich *et. al.*(1997). This process, which may seem quite dissimilar to conventional batch milling, can nevertheless be described by the batch comminution equation if the progeny are subject to sequential rebreakage after initial breakage of individual particles. The Schneider model of the attainable region was modified using equation (35). Fandrich *et. al.* also found evidence of differential breakage by measuring the variation of the size breakage function $b_{j,kl}$ with particle composition and they modeled this effect using a truncated log normal model for the breakage function. Their model for the size breakage function was used here and the variation of particle grade with particle size in the product was calculated for the five monograde-monosize feeds that were used in their experiments. The calculated results are compared with the experimental data in Figure 7. It is clear that the theoretical model is capable of describing the effects of preferential and differential breakage satisfactorily.

CONCLUSIONS

The general solution to the multicomponent batch comminution (equation (19)) can be used to calculate the liberation spectra as a function of particle size in the products from a batch grinding mill. Both random and non-random breakage effects can be modeled. Selective breakage can be simulated by modeling the effect of unequal mineral brittleness on the selection function. Preferential breakage can be simulated through its effect on the internal and possibly also on the boundary structure of the attainable region. Differential breakage can be simulated using experimentally determined variations in the size breakage function with parent particle composition.

The selective breakage model use here (Equation 32) is only a tentative attempt to examine the consequence of selective breakage. A considerable amount of careful experimental work will be required to quantify all the effects of non-random fracture. (See Choi *et. al* 1988 for example).

The solutions developed in this paper provide effective methods for the determination of the essential parameters to model the effects of mineral liberation in industrial grinding mills.

The mode of stress application in the grinding mill can influence the liberation characteristics of an ore. Fandrich *et. al.* (1997) for example have put forward an interesting argument for increased

selective breakage when a particle is stressed within a constrained particle bed as opposed to stressing between two metal surfaces. Factors such as this must be taken into account when transferring model parameters determined in laboratory experiments to plant scale operations.

ACKNOWLEDGMENTS

This work was supported by the Department of the Interior through the Generic Mineral Technology Center for Comminution under grant G-115249 and by the Department of Energy under grant number DE-FG22-95PC95220 and by the State of Utah under its Center of Excellence Program.

REFERENCES

Andrews J. R. and Mika, T., (1975) Comminution of heterogeneous material; development of a model for liberation phenomena. *Proc. 11th Intl. Mineral Processing Congress*, Cagliari, pp 59-88.

Choi, W.Z., Adel, G.T. and Yoon, R.H., (1988) "Liberation modeling using automated image analysis". *Intl. Jnl. Mineral Processing 22*, pp 59-73.

Fandrich, R., G., Bearman, R., A., Boland, J. and Lim, W. (1997) Mineral liberation by particle bed breakage. *Minerals Engineering*, 10, 175 -187.

Gaudin, A. M. (1939). Principles of Mineral Dressing. McGraw-Hill.

King R.P. (1972) An analytical solution to the batch-comminution equation. *Jnl. S. Afr. Inst, Mining Metall.* 73 pp 127-131.

King, R.P, (1990) Calculation of the liberation spectrum in products produced in continuous milling circuits. *Proc. 7th European Symposium on Comminution*, Ljubljana, Vol 2 pp 429-444.

King, R., P. (1994) Linear stochastic models for liberation. *Powder Technology* 81, 217-234

King, R.P. and Schneider, C., (1993) Mineral Liberation in continuous milling circuits. *Procs. XVIII International Mineral Processing Congress*, Aus. Inst. Mining Metall.

King R. P. and Schneider C.L. (1998) Stereological correction of linear grade distributions for mineral liberation. *Powder Technology*. In print.

Liu, J., and Schönert, K. (1996) Modelling of interparticle breakage. *Intl. Jnl. Mineral Processing.* 44-45, 101-115

Middlemiss, S. and King, R., P. (1996) Microscale fracture measurements with applications to

comminution. Intl. Jnl. Mineral Processing, 44-45, 43-58.

Nakajima, Y., and Tanaka, T. (1973). Solution of batch grinding equation. *Ind. Eng. Chem., Process Design Dev.* 12, pp23-25.

Schneider, C., L., (1995) Measurement ans Calculation of Liberation in Continuous Milling Circuits. PhD thesis, university of Utah. Available by FTP at ftp://www.mines.utah.edu/Pub/Cmt/

Wiegel, R.L., (1976) Integrated size reduction-mineral liberation model. *Trans. Soc. Mining Engrs. 260*, pp147-152.

APPENDIX - CONDITIONS THAT ENSURE CONSERVATION OF EACH SPECIES

The average grade of mineral in the total population of particles in the batch mill must remain invariant with time to ensure conservation of mass of each species. Thus

$$\frac{\partial}{\partial t}\int_0^\infty\int_0^1 g\,p(g,D)\,dg\,dD = 0 \tag{39}$$

Equation (8) can be written in differential form as

$$\frac{\partial p(g,D;t)}{\partial t} = -S(g,D)\,p(g,D;t) + \iint_{R'} b(g,D|g',D')\,S(g',D')\,p(g',D')\,dg'\,dD' \tag{40}$$

Multiplying this equation by g and integrating gives

$$\begin{aligned}\frac{\partial}{\partial t}\int_0^\infty\int_0^1 g\,p(g,D)dg\,dD &= -\int_0^\infty\int_0^1 gS(g,D)\,p(g,D)\,dg\,dD \\ &+ \int_0^\infty\int_0^1 S(g',D')\,p(g',D')\int_{g*}^{g**}\int_0^{D'} g\,b(g,D|g',D')\,dD\,dg\,dg'\,dD'\end{aligned} \tag{41}$$

A sufficient condition for equation (39) to be satisfied is therefore

$$\int_{g*}^{g**}\int_0^{D'} g\,b(g,D|g',D')\,dD\,dg = g' \qquad \text{for all } g' \text{ and } D' \tag{42}$$

$g*$ and $g**$ represent the left and right hand boundaries of the attainable region at each value of D

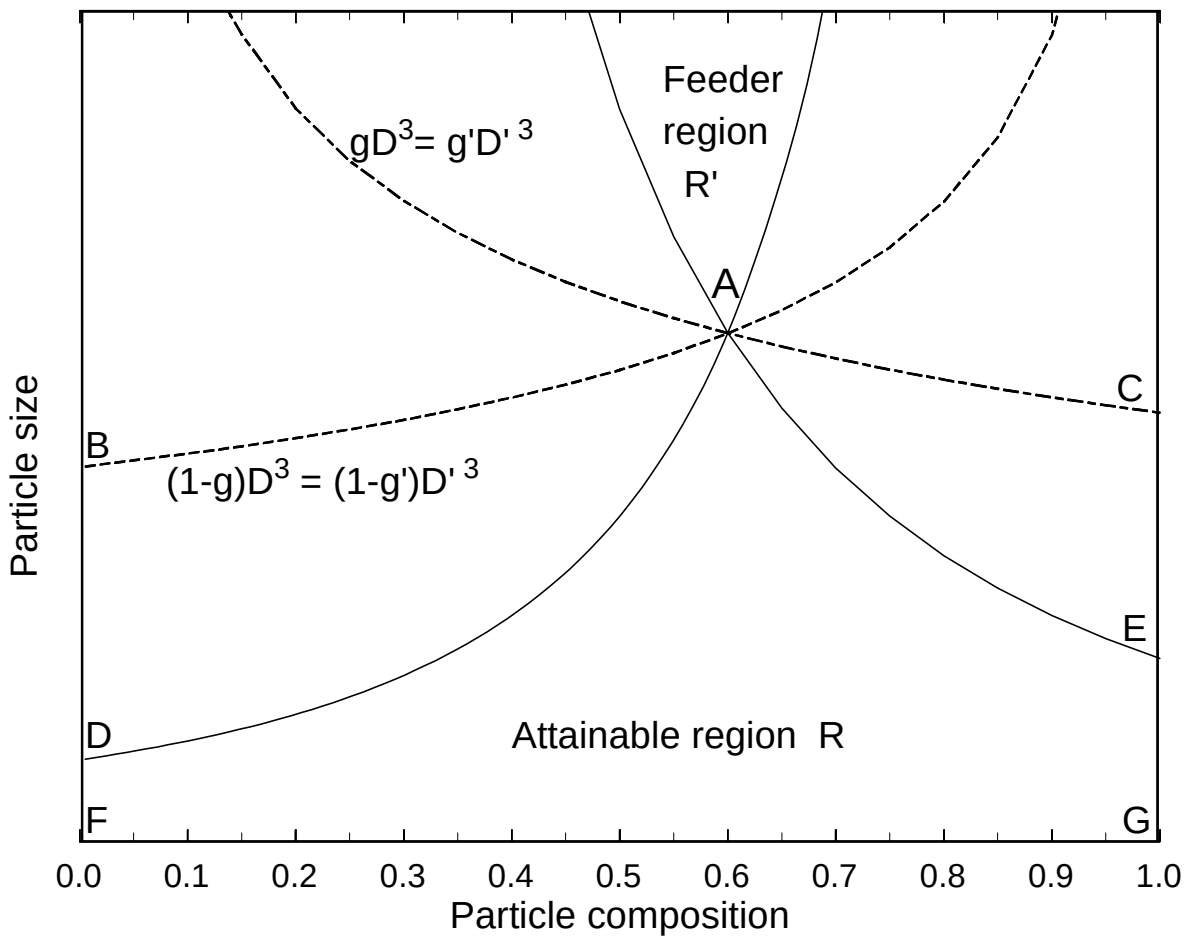

Figure 1 Boundaries of the Andrews-Mika diagram showing both the feeder region R′ and the attainable region R.

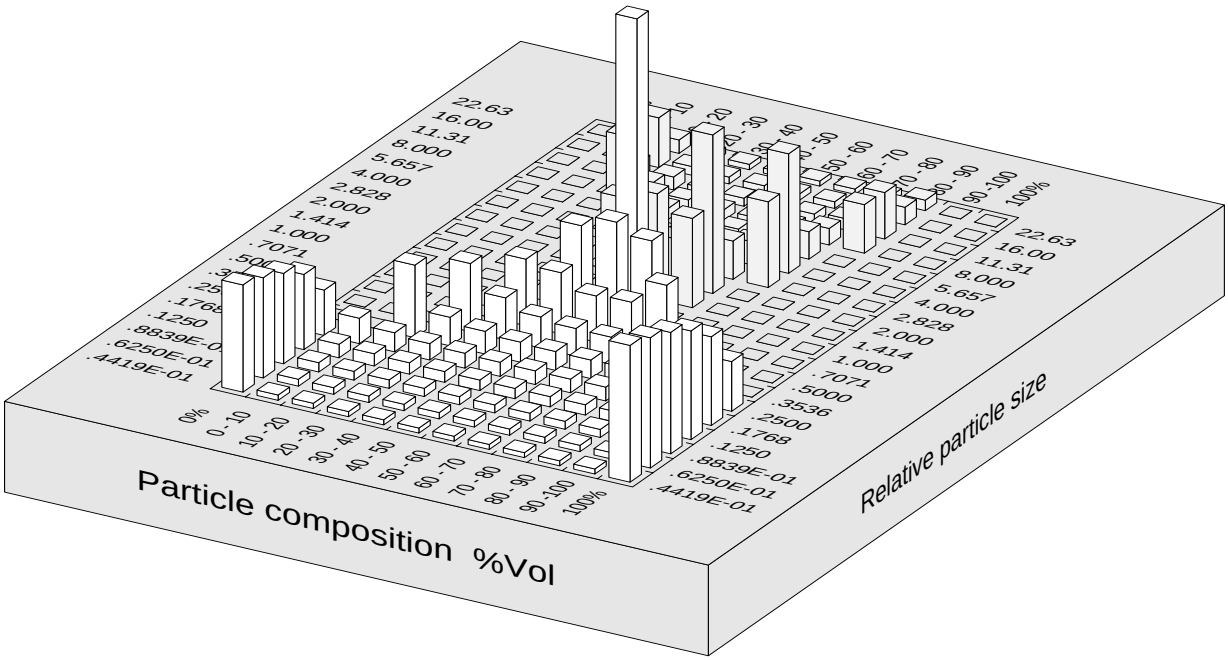

Figure 2 Internal structure of a typical Andrews-Mika diagram showing both the feeder and attainable regions. The feeder region is indicated by the shaded bars in the upper half of the diagram and the attainable region is indicated by the unshaded bars in the lower half of the diagram. The height of each bar in the feeder region represents the conditional multicomponent breakage function $b_{7,10kl}$ where k and l represent any parent bar in the feeder region.

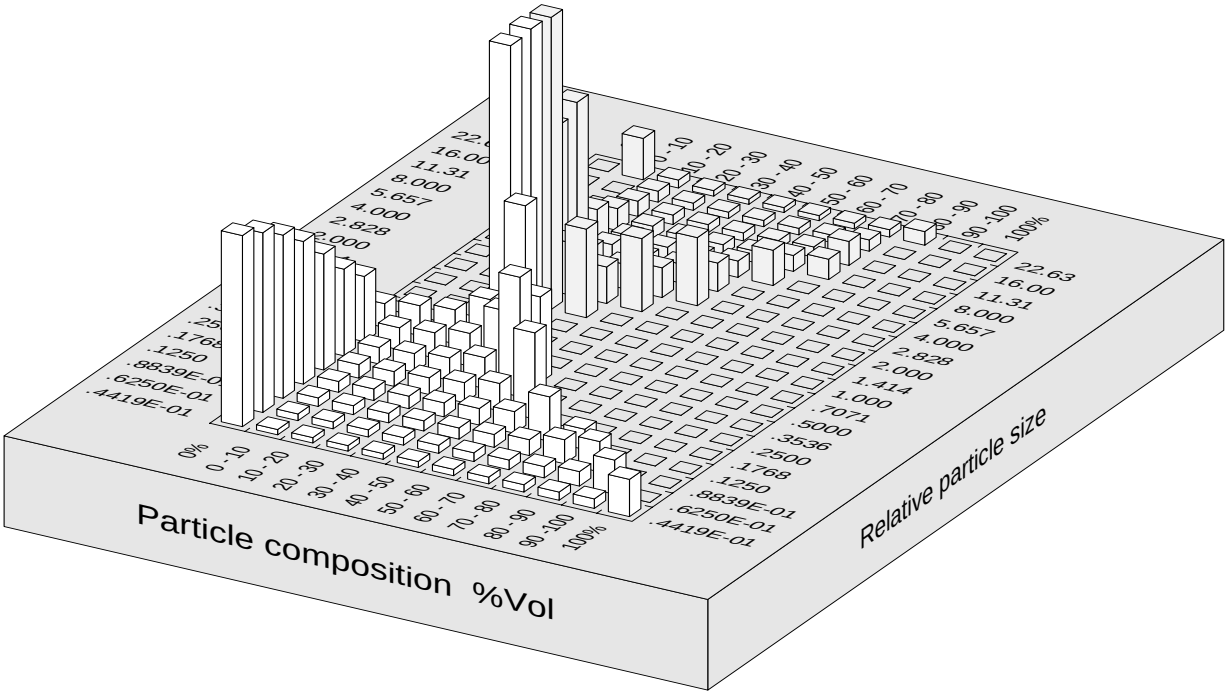

Figure 3 Internal structure of a typical Andrews-Mika diagram showing both the feeder and attainable regions. The feeder region is indicated by the shaded bars in the upper half of the diagram and the attainable region is indicated by the unshaded bars in the lower half of the diagram. The height of each bar in the feeder region represents the conditional multicomponent breakage function $b_{4,10kl}$ where k and l represent any parent bar in the feeder region.

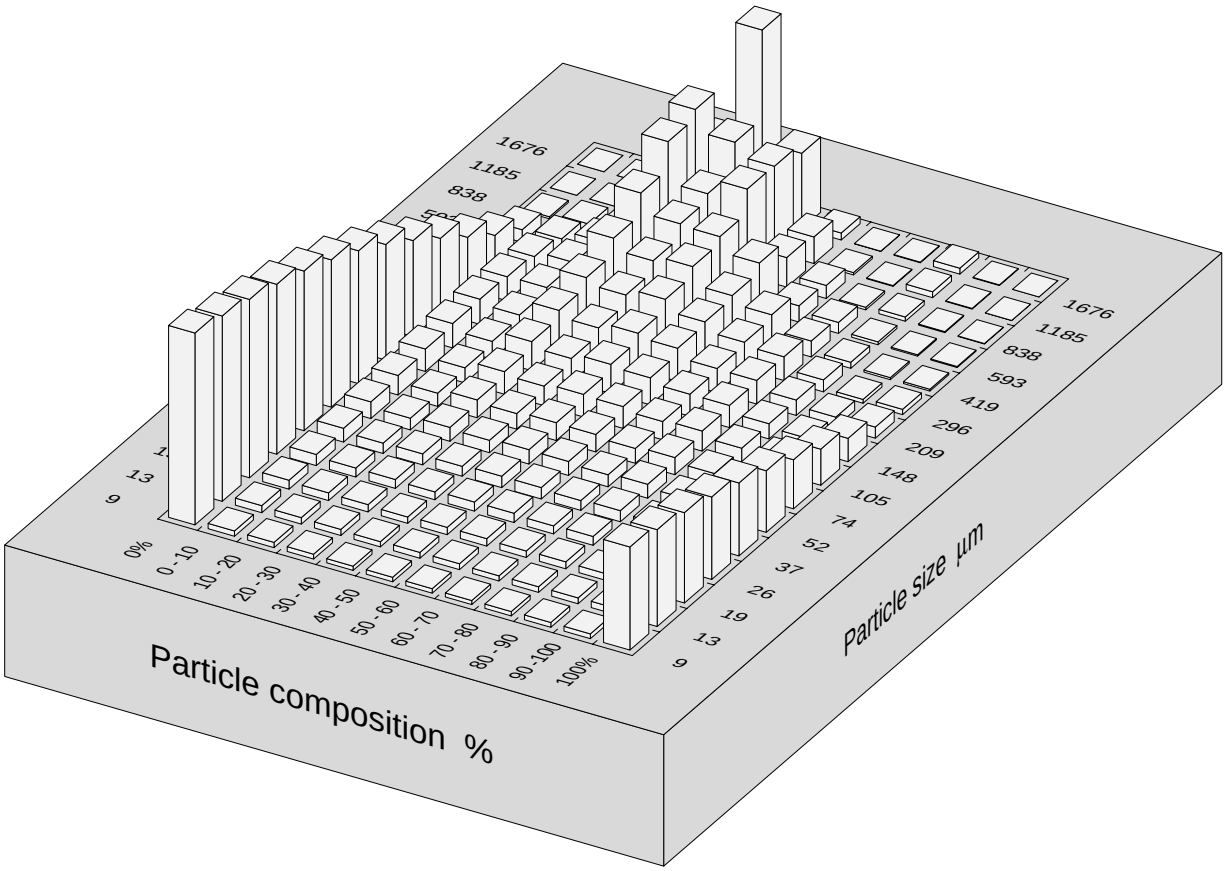

Figure 4 Calculated liberation spectra after 10 minutes of batch grinding. These spectra do not change significantly with grinding time after an initial transient period.

am10mfal.txt

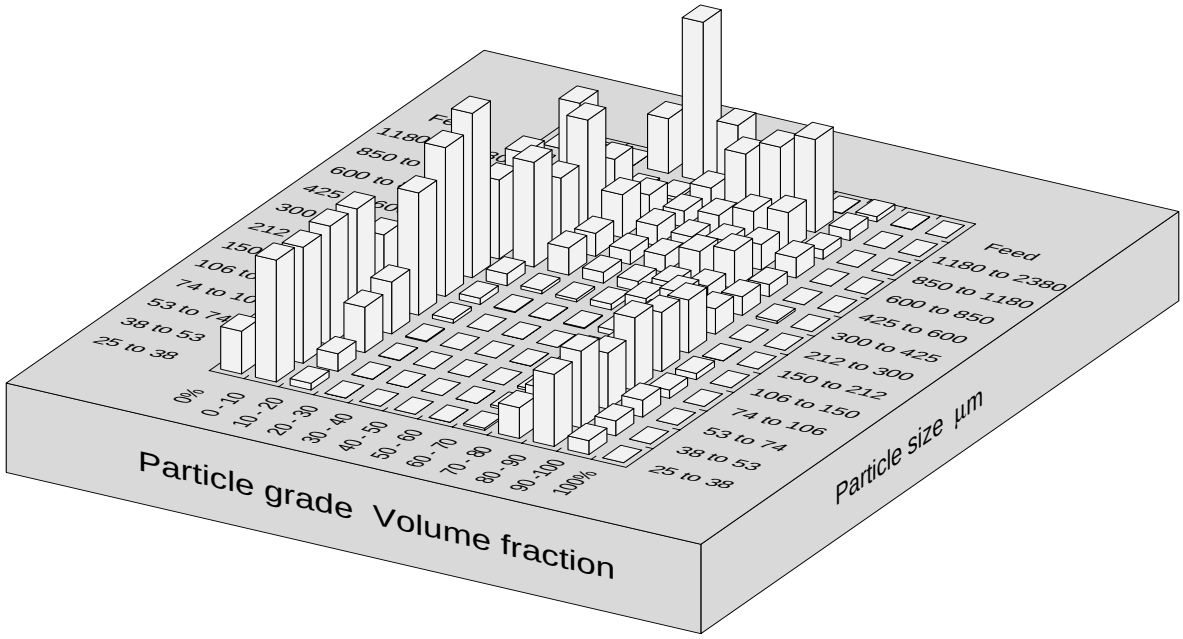

Figure 5 Measured liberation spectra after 10 minutes grinding of an iron ore.

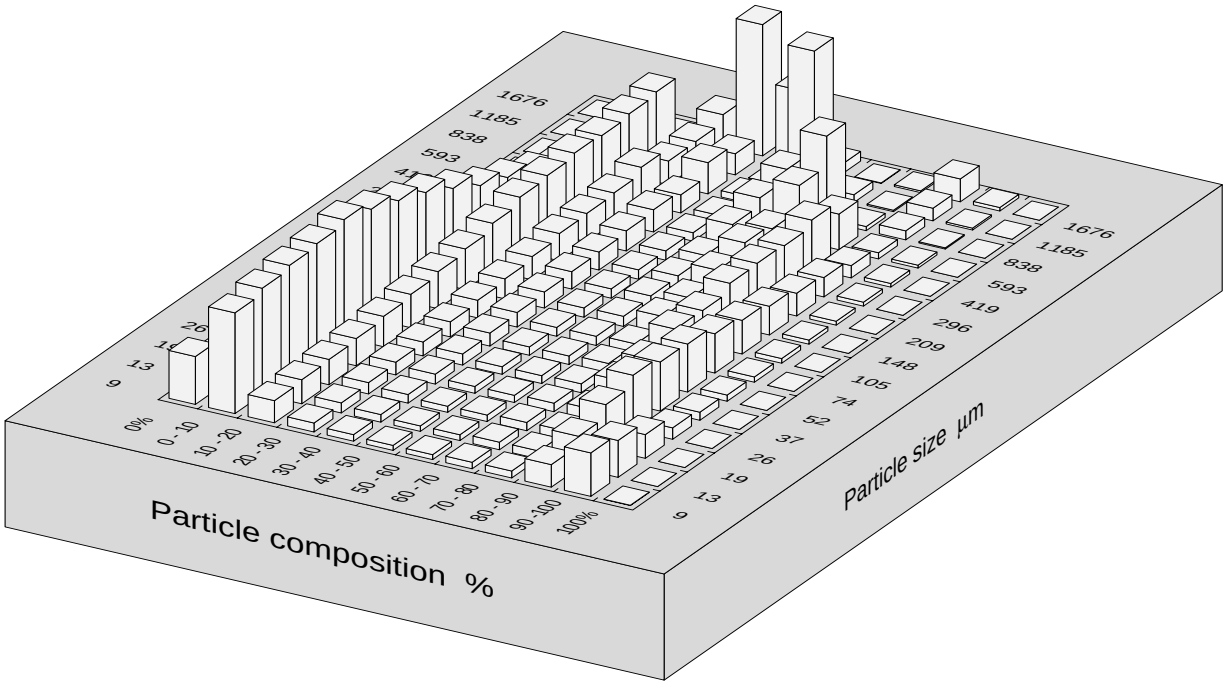

Figure 6 Calculated liberation spectra after 10 minutes grinding using the Andrews-Mika diagram for this ore and assuming a brittleness ratio of 0.5

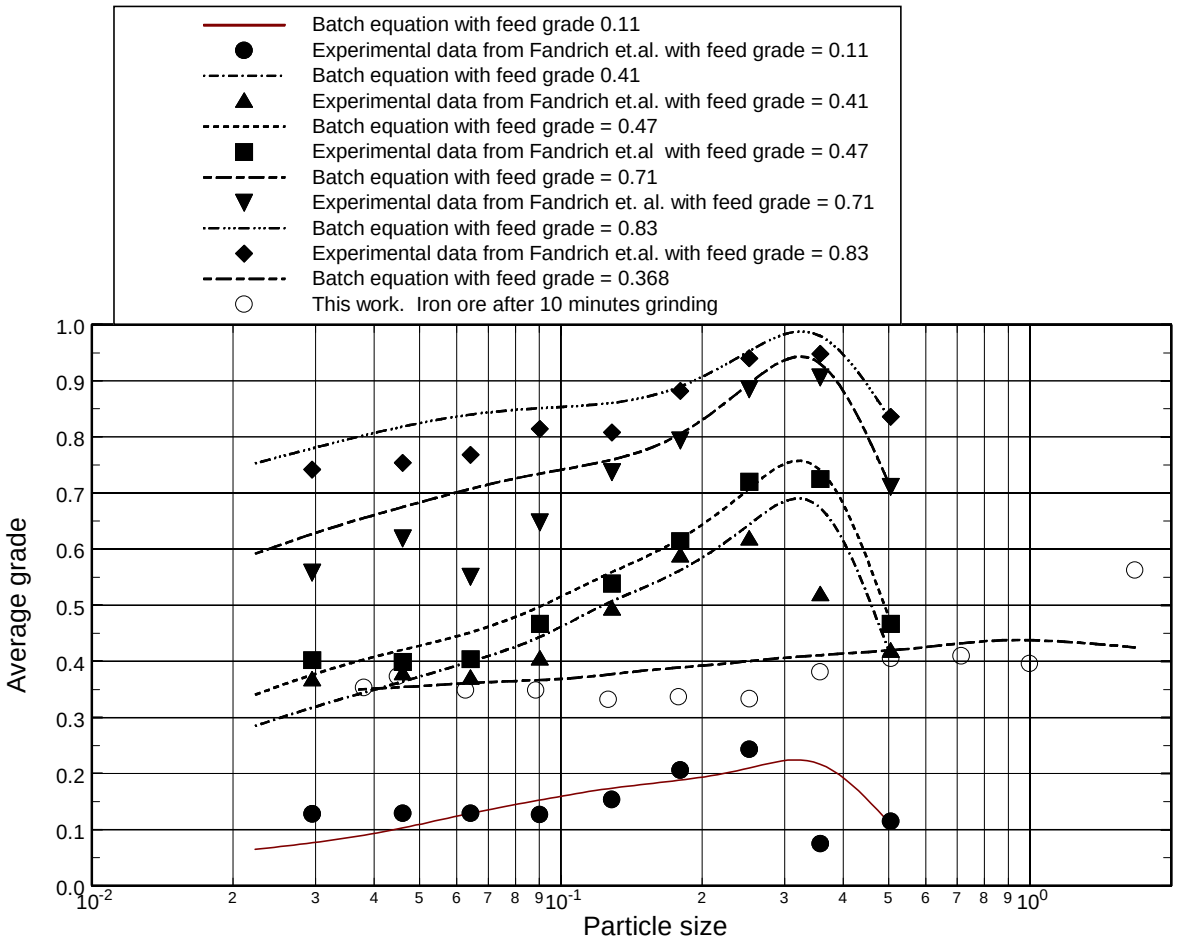

Figure 7 Calculated variation of average grade with size compared with measured data of Fandrich *et. al.*(1997). Calculated values show the effects of preferential and differential breakage (filled symbols) and the effect of selective breakage(open symbols).

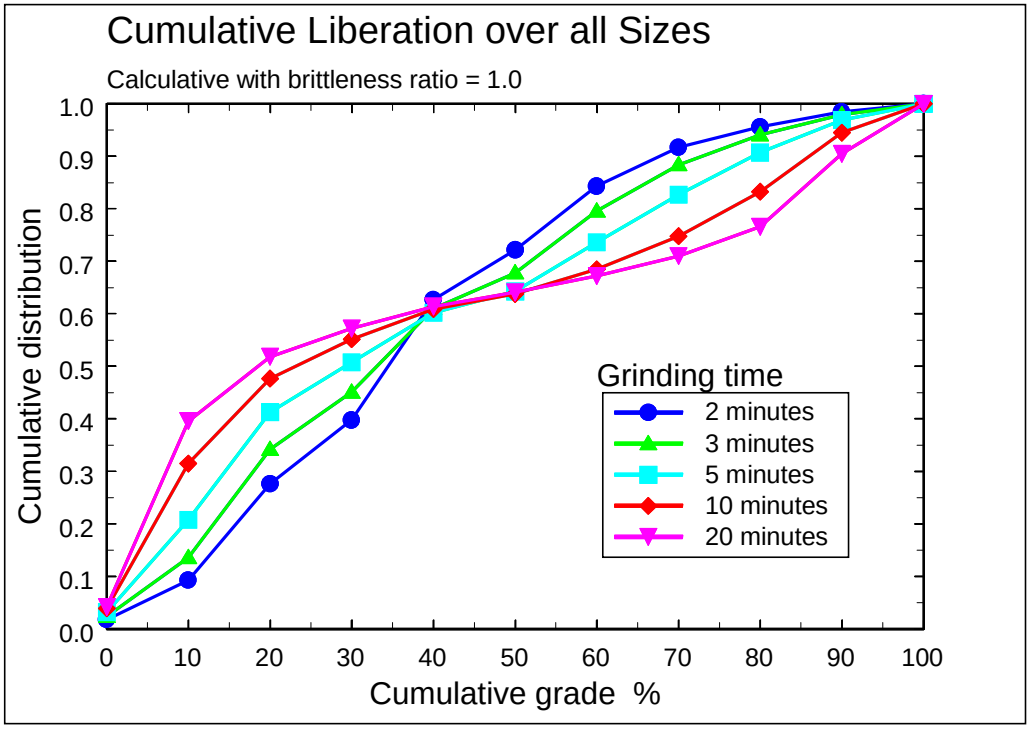

Figure 8 Calculated cumulative liberation distributions averaged over all sizes at 5 different grinding times with no selective breakage.

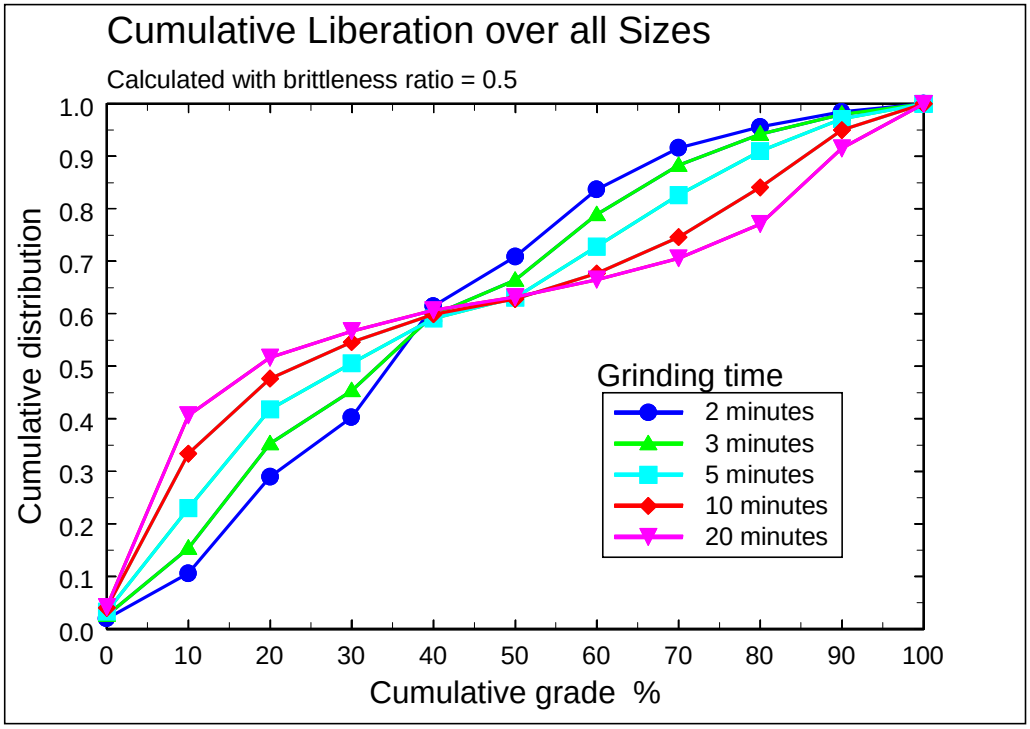

Figure 9 Calculated cumulative liberation distributions averaged over all sizes at 5 different grinding times with selective breakage of the gangue.